Proc. Natl. Acad. Sci. USA
Vol. 76, No. 1, pp. 232–235, January 1979
Biochemistry

Coupled enzyme systems in a vesicular membrane: Oxidative phosphorylation as an example

(ligand transport/steady-state kinetics/respiratory control)

TERRELL L. HILL

Laboratory of Molecular Biology, National Institute of Arthritis, Metabolism and Digestive Diseases, National Institutes of Health, Bethesda, Maryland 20014

Contributed by Terrell L. Hill, November 2, 1978

ABSTRACT **We consider a small vesicle whose membrane transports a ligand L into the vesicle through enzymatic units of type A and transports L out of the vesicle through units of type B. Oxidative phosphorylation in mitochondria provides an example, in which L is H^+. The kinetics of the two membrane systems (A and B) are coupled through the concentration of L in the vesicle. This interdependence causes the combined membrane system (A plus B) to simulate a single system whenever the net ligand transport into the vesicle is zero. For example, in oxidative phosphorylation, it was thought for some time that ATP was synthesized by the respiratory chain system (via an "active intermediate"). We give the simplest possible analysis of this kind of coupled system, which is very common, by using two-state enzymes for both A and B above. A numerical example is included that illustrates respiratory control in a qualitative way: although the respiratory chain flux by itself does not depend on ADP concentration, the steady-state flux of the *coupled* systems (respiratory chain and reverse ATPase) does depend on ADP concentration through the interior ligand (H^+) concentration.**

In recent papers we have considered the steady-state kinetics of aggregates of enzyme molecules that interact with each other either through nearest-neighbor free energy effects (1–5) or by means of interlocking reactions (5–7). In this paper we treat, as a prototype, a very simple model that illustrates a quite different type of enzyme interaction. Suppose we have a small vesicle, natural or synthetic, of volume V, with two kinds of enzyme molecules (or complexes or units) embedded in the vesicular membrane. There are M_A molecules of type A and M_B of type B. Each of these units behaves independently of the rest except for the fact that units of type A transport a ligand L from outside the vesicle to inside whereas units of type B transport L from inside to outside. Because V is small and the inside ligand concentration is responsive to the ligand transport, the shared ligand has the effect of coupling the A and B systems to each other in a rather sensitive way. We examine this coupling here assuming that both A and B units can be treated as two-state enzyme molecules. An adequate representation of real units would generally require the use of more states than this; furthermore, natural vesicles (e.g., mitochondria) might have more than two kinds of membrane units coupled through the same ligand (e.g., H^+); see below. However, we do not treat these generalizations here.

In a formal way, let us write the complete process catalyzed by A molecules as

$$L_{out} + P_A \rightarrow L_{in} + S_A;\ X_A \qquad [1]$$

and by B molecules as

$$L_{in} + S_B \rightarrow L_{out} + P_B;\ X_B \qquad [2]$$

where S refers to substrate, P to product, and X to the net thermodynamic force. At steady state, when the inward ligand transport by A units is just balanced by the outward ligand transport by B units, the over-all process is

$$S_B + P_A \rightarrow P_B + S_A;\ X_A + X_B. \qquad [3]$$

To choose an explicit case (suggested by oxidative phosphorylation), we assume that the "downhill" L gradient out → in is large enough to drive the "backward" reaction $P_A \rightarrow S_A$ (the former has a positive thermodynamic force, the latter has a negative force, while the net force X_A is positive). Similarly, we assume that $S_B \rightarrow P_B$ (positive force) is able to drive L up its gradient (in → out; negative force) with a net positive force X_B. In the oxidative phosphorylation example (ignoring stoichiometry), the vesicle interior is the mitochondrial matrix, the L gradient is the proton electrochemical gradient, an A unit is the reverse ATPase complex (P_A is ADP,P_i; S_A is ATP), and a B unit is a "transducing site" region of the respiratory chain complex (S_B refers to electron donor and acceptor; P_B refers to oxidized donor and reduced acceptor). Recent work (8) shows that a third kind of membrane unit (see above), involved with ATP-ADP exchange, is also coupled through protons. This is ignored here. A more detailed treatment would simply include two kinds of A units.

Formal kinetics of coupled two-state molecules

In this section we derive the simple general properties of the coupled two-state units in terms of the rate constants of the model. In the next section we introduce explicit, illustrative, multi-state biochemical cycles for the example of oxidative phosphorylation in order to lend some molecular reality to the two-state cycles used here. In the final section, we present a two-state numerical example that illustrates respiratory control in a qualitative way.

Figs. 1 and 2 should be examined together. Fig. 1 shows several A and B enzyme units schematically (● and x, respectively), with only the ligand (○), not substrates and products, appearing explicitly in the figure. State 2 (for both A and B) has ligand bound; state 1 has ligand not bound. The relation of these states to more complete biochemical cycles will be illustrated in the next section. In general, with two-state cycles, it is to be understood that more complicated cycles have been "reduced" (ref. 5, appendix 1) because of transient intermediates, etc.

The same rate constants appear in both Figs. 1 and 2. The associated physical processes (binding or release of ligand) are indicated in Fig. 1, whereas the kinetic cycles are shown in Fig. 2. Unprimed rate constants are usually the dominant ones (counterclockwise in Fig. 2); the smaller inverse rate constants are primed. An asterisk indicates a second-order rate constant; the others are first-order or pseudo first-order rate constants. The interior concentration of ligand is $c = N/V$; because V is small, c cannot be treated as a constant. However, for simplicity, we assume that ligand is maintained at a constant *exterior*

The publication costs of this article were defrayed in part by page charge payment. This article must therefore be hereby marked "*advertisement*" in accordance with 18 U. S. C. §1734 solely to indicate this fact.

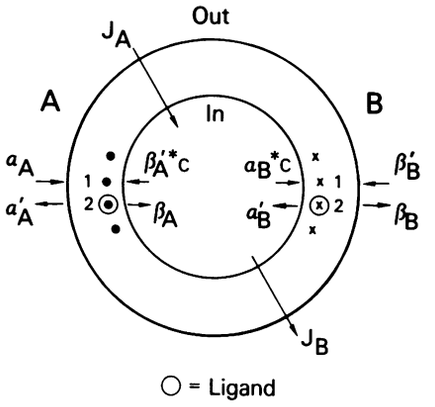

FIG. 1. Schematic vesicle with membrane. Units of type A(●) and B(x) transport a ligand L(○) across the vesicular membrane. Interior concentration of L is c. Arrows indicate binding or release of ligand. See text.

concentration over the time period of interest. Also, for clarity and simplicity, we assume that substrates and products are maintained at constant concentrations wherever they appear (inside or out). The membrane potential, if involved, is also assumed to be constant. In the reverse ATPase case (above), for example, the interior ADP, P_i, and ATP concentrations could be kept essentially constant by the separate phosphate and ADP-ATP carrier systems (9) that are also present in the mitochondrial inner membrane. It is because of the above mentioned simplifying assumptions that no other second-order rate constants are used in Figs. 1 and 2. The constant concentrations referred to above are "imbedded" in pseudo first-order rate constants, one way or another (ref. 5, appendix 1).

The fraction of A units in state 1 is denoted by p_A, etc. (Fig. 2). The kinetic equations for the variables p_A, p_B, and c are

$$\frac{dp_A}{dt} = (\alpha'_A + \beta_A)(1 - p_A) - (\alpha_A + \beta'^*_A c)p_A \quad [4]$$

$$\frac{dp_B}{dt} = (\alpha'_B + \beta_B)(1 - p_B) - (\alpha^*_B c + \beta'_B)p_B \quad [5]$$

$$\frac{dc}{dt} = \frac{M_A}{V}[\beta_A(1 - p_A) - \beta'^*_A c p_A] + \frac{M_B}{V}[\alpha'_B(1 - p_B) - \alpha^*_B c p_B]. \quad [6]$$

We are interested, primarily, in the steady state. For this, let us consider first the *hypothetical separate* steady states of A and B units for an arbitrary value of c. We find (5) for the fluxes J_A

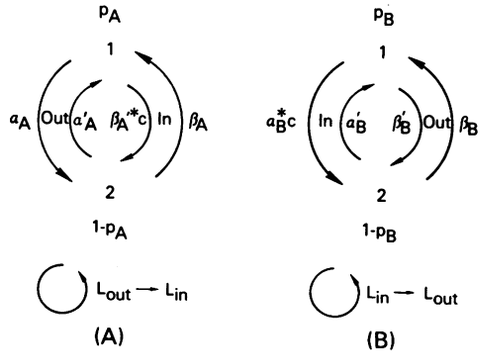

FIG. 2. Two-state cycles for A (A) and B (B) units, with first-order rate constant notation for transitions (arrows). Dominant cycle direction is counterclockwise in both cases. "Out" refers to binding and release of ligand to exterior, etc. See text.

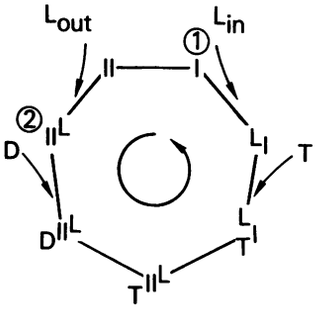

FIG. 3. Seven-state cycle for reverse ATPase that could serve as precursor of Fig. 2A. See text for notation.

and J_B (Fig. 1)

$$J_A(c) = \frac{M_A(\alpha_A\beta_A - \alpha'_A\beta'^*_A c)}{\alpha'_A + \beta_A + \alpha_A + \beta'^*_A c}, \quad [7]$$

$$J_B(c) = \frac{M_B(\alpha^*_B c\beta_B - \alpha'_B\beta'_B)}{\alpha'_B + \beta_B + \alpha^*_B c + \beta'_B}. \quad [8]$$

These are not only the ligand fluxes but also the fluxes of substrates and products involved in the two cycles.

Incidentally, if only A units or only B units were present in the membrane, c would be free to adjust itself to the corresponding equilibrium value:

$$J_A(c^A_e) = 0,\ c^A_e = \alpha_A\beta_A/\alpha'_A\beta'^*_A \quad [9]$$

$$J_B(c^B_e) = 0,\ c^B_e = \alpha'_B\beta'_B/\alpha^*_B\beta_B. \quad [10]$$

Note, in Eqs. 7 and 8, that $J_A(c)$ starts ($c = 0$) from a positive value and ends ($c = \infty$) at a negative value, while $J_B(c)$ does the reverse. That is, J_A decreases and J_B increases with increasing c; the latter dependence on c is usually stronger because an unprimed rate constant is involved. The two curves necessarily cross each other. The intersection occurs at the steady-state value of c, c_∞, determined by $J_A(c_\infty) = J_B(c_\infty)$ (Eqs. 7 and 8). This is, in effect, the desired steady-state solution of Eqs. 4 through 6. $J_A = J_B$ leads to a quadratic equation in c_∞, which we omit. We denote the steady-state flux $J_A = J_B$ by J_∞. This flux will be positive if $c^A_e > c^B_e$ (the usual case; note the primes in Eqs. 9 and 10). The last section provides an explicit numerical example. The A and B systems are coupled to each other, at steady state, through their common dependence on the value of c_∞ in the small volume V.

There are special cases (e.g., one-way cycles) for which the quadratic equation in c_∞, above, becomes linear, but we leave these to the interested reader.

If the rate constants happen to be such (Eqs. 9 and 10) that $c^A_e = c^B_e$, then this is also the value of c_∞, and $J_\infty = 0$. In this special case, the steady state is an equilibrium state (for both A and B).

The steady-state thermodynamic forces X_A and X_B are given by

$$e^{X_A/kT} = \alpha_A\beta_A/\alpha'_A\beta'^*_A c_\infty,\ e^{X_B/kT} = \alpha^*_B c_\infty\beta_B/\alpha'_B\beta'_B. \quad [11]$$

Both X_A and X_B are usually positive; each is a combination of two subforces (Eqs. 1 and 2). Because $J_A = J_B$ at steady state, there is no net ligand transport in the coupled system (A plus B) and the sum $X_A + X_B$, determined by

$$e^{(X_A+X_B)/kT} = \alpha_A\beta_A\alpha^*_B\beta_B/\alpha'_A\beta'^*_A\alpha'_B\beta'_B, \quad [12]$$

has the physical significance indicated in Eq. 3. Note that c_∞ does not appear in Eq. 12. Operationally (i.e., viewed as a "black box"), the coupled A and B systems simulate a *single* kind of system with flux J_∞, force $X_A + X_B$, and net reaction given by

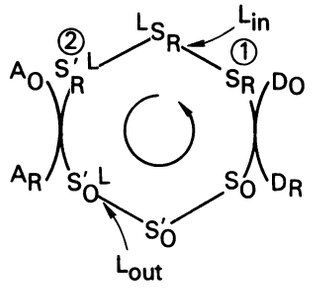

FIG. 4. Six-state cycle for respiratory chain "transducing site" enzyme that could serve as precursor of Fig. 2*B*. See text for notation.

Eq. 3. Even though $M_A \neq M_B$, the stoichiometry in Eq. 3 is precise because $J_A = J_B$. At this level, the role of the ligand does not appear explicitly. These comments seem pertinent to the history of the study of oxidative phosphorylation (9): until rather recently, perhaps because of the simulation of a single kind of system, ATP was generally thought to be synthesized by the respiratory chain, via an "active intermediate" (rather than by a separate reverse ATPase system).

We confine our brief discussion of the subject of transients to two limiting cases. From Eqs. 4 through 6, we have the following *order of magnitude* equations, writing p for p_A or p_B, M for M_A or M_B, and α for a first-order rate constant:

$$\Delta p = \alpha p \Delta t,\ \Delta c = (M/V)\Delta p,\ \Delta c/c = (M/N)\Delta p, \quad [13]$$

where Δt is a small time interval and N is the number of ligand molecules in V.

(*i*) If $N \gg M$, c changes fractionally much more slowly than p changes. In this case, each of systems A and B (Eqs. 4 and 5) quickly comes to its own steady state appropriate to the relatively slowly changing value of c. In fact, the two steady-state fluxes at any c are given by Eqs. 7 and 8, and Eq. 6 can be written

$$dc/dt = [J_A(c) - J_B(c)]/V. \quad [14]$$

Mathematically, then, we are left with a single differential equation in c, Eq. 14. This case arises, for example, if V is large, because $N = cV$.

(*ii*) If $M \gg N$, c will quickly come to and maintain a steady-state value appropriate to the relatively slowly changing values of p_A and p_B. The value of c, at any t, will be such as to give zero net flux of ligand into the vesicle. We set the right-hand side of Eq. 6 equal to zero, solve for c, and put this expression in place of c in Eqs. 4 and 5. We are left, then, with two differential equations in p_A and p_B. In a typical mitochondrion, which has both a small c and a small volume (9), N (number of protons) is of order 10^2 whereas M is of order 10^4. Hence this case ($M \gg N$) applies.

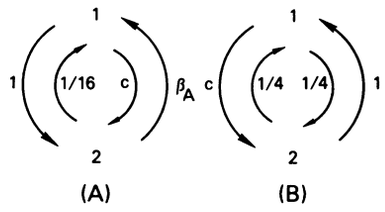

FIG. 5. Rate constant assignment for Fig. 2 in numerical example. See text.

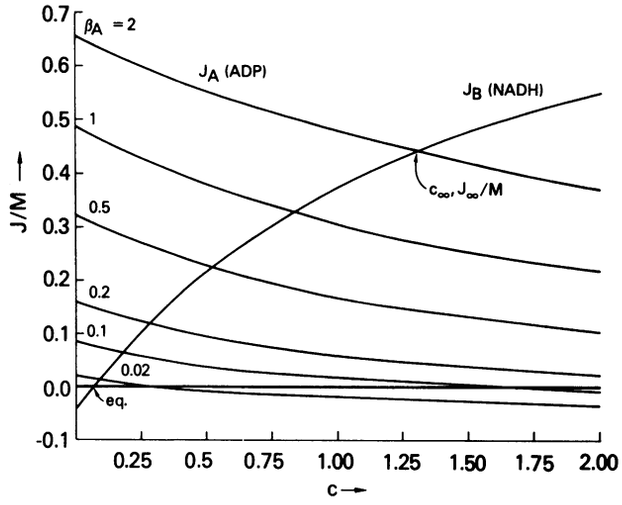

FIG. 6. Plot of J_A/M and J_B/M against c, for several values of β_A, for numerical example in Fig. 5. Intersection points give steady-state values of J_∞/M and c_∞. Equilibrium point is labeled "eq".

Illustrative biochemical cycles

To give some molecular significance to the formal two-state cycles in Fig. 2, we discuss here more detailed biochemical cycles that could serve as the precursors of Fig. 2. This is done for the case of oxidative phosphorylation. However, the cycles chosen are not to be taken seriously (e.g., they ignore the real stoichiometry). Their purpose is primarily pedagogical.

Thus the seven-state cycle in Fig. 3 might be the source of the two-state cycle in Fig. 2*A*, by reduction of the larger cycle (ref. 5, appendix 1). [Incidentally, the actual seven-state myosin ATPase cycle does reduce, effectively, to a two-state cycle (see ref. 5, p. 83)]. The model and notation here are taken from earlier papers (10, 11). I and II in Fig. 3 represent two conformations of the enzyme. Also, L is H^+, T is ATP, and D is ADP + P_i. The bound ligand has access to the inside (left superscript) when the enzyme is in conformation I and to the outside (right superscript) in conformation II. The dominant direction of the cycle is counterclockwise (as in Fig. 2*A*). The out → in H^+ gradient drives the synthesis of T from D. In Eq. 1, P_A is D and S_A is T.

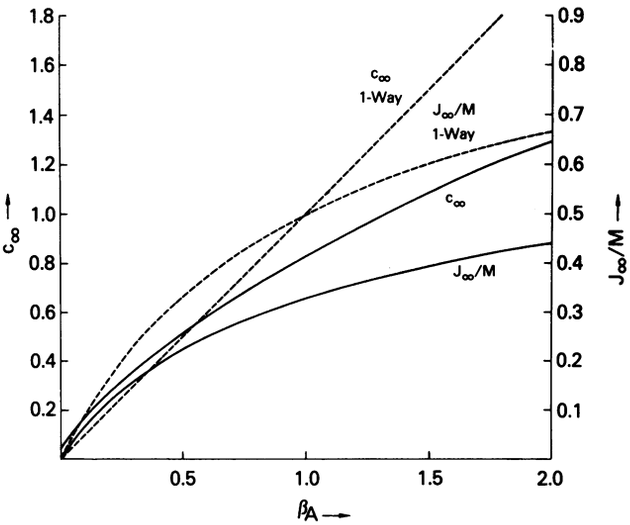

FIG. 7. Plots of J_∞/M and c_∞ against β_A, taken from intersection points in Fig. 6. The flux represents qualitatively the dependence of the rate of oxygen uptake and ATP synthesis on ADP concentration (β_A). Dashed curves are for one-way special cases.

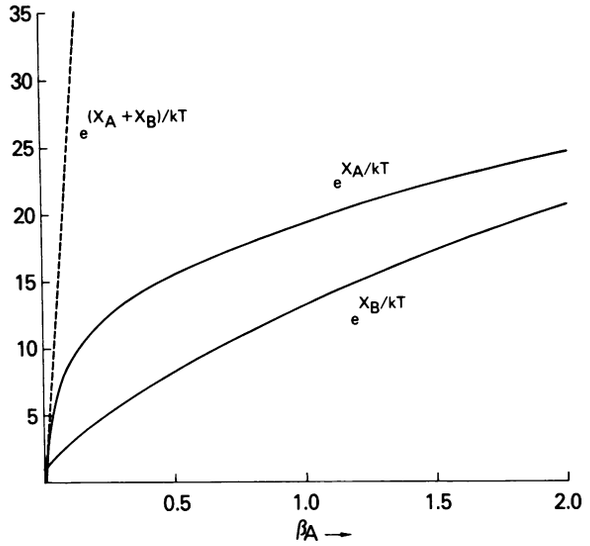

FIG. 8. Plots of thermodynamic forces (X) against β_A at steady state, in numerical example. See text.

If, for example, we assign states 1 and 2 as indicated by the circled numbers in Fig. 3, the expression $\beta_A^* c$ in Fig. 2*A* is accounted for by the L_{in} arrow in Fig. 3. Note also that β_A in Fig. 2*A* would be (according to Fig. 3) proportional to the fixed concentration of D. In the next section we consider variations in the fixed ADP concentration.

Fig. 4 (a possible source of Fig. 2*B*) shows a hypothetical six-state cycle for a respiratory chain "site" enzyme S. The notation is taken from ref. 6. The enzyme has two conformations, S and S′. Also, L is H^+, R means reduced, O means oxidized, A means acceptor, and D means donor. L has access to the inside when bound to S and to the outside when bound to S′. The dominant cycle direction is counterclockwise (as in Fig. 2*B*): the reaction $D_R + A_O \rightarrow D_O + A_R$ drives L in → out against its gradient. In Eq. 2, S_B is $D_R + A_O$ and P_B is $D_O + A_R$. The assignment of states 1 and 2 is included in Fig. 4. The L_{in} arrow in this figure accounts for the expression $\alpha_B^* c$ in Fig. 2*B*.

Numerical example: respiratory control

We now provide a numerical illustration of the steady state properties of the coupled two-state systems in Fig. 2. For convenience, the rate constants and c are chosen to be dimensionless and of order unity, as shown in Fig. 5. Also, we take $M_A = M_B \equiv M$. If we adopt the biochemical interpretation in the preceding section, the example allows a qualitative understanding of respiratory control (9). That is, system A in Fig. 5 is the reverse ATPase and β_A is proportional to the fixed but adjustable ADP concentration (holding P_i constant). Our object is to see how the steady state of the coupled system, especially the flux J_∞ (proportional to the rate of oxygen uptake or ATP synthesis), depends on the assigned β_A (i.e., ADP) level.

For any choice of β_A, the steady state can be determined as in Fig. 6. Here we plot $J_A(c)/M$ and $J_B(c)/M$ from Eqs. 7 and 8, using the rate constants in Fig. 5 and several values of β_A. The points of intersection determine J_∞/M and c_∞. Although $J_B(c)$ (respiratory chain) itself is independent of β_A (i.e., ADP), the steady-state flux J_∞ of *both* systems (A and B) is clearly fairly sensitive to β_A, because of the coupling of the two systems through the interior ligand concentration c. Fig. 7 presents J_∞/M and c_∞ as functions of β_A (from the intersection points in Fig. 6). The flux $J_\infty(\beta_A)/M$ simulates that of a single system. For large β_A,

$$J_\infty/M \rightarrow a\beta_A^{1/2}/(1 + a\beta_A^{1/2}) \qquad [15]$$

where $a = (2/3)^{1/2}$. The equilibrium point in Fig. 6 (labeled "eq.") has $\beta_A = 1/256$, $c_\infty = 1/16$, and $J_\infty = 0$.

For comparison, in Fig. 7, we include (dashed lines) the one-way special case (the clockwise rate constants in Fig. 5 are set equal to zero). Here $c_\infty = \beta_A$ and $J_\infty/M = \beta_A/(1 + \beta_A)$.

Fig. 8 gives the force functions

$$e^{X_A/kT} = 16\beta_A/c_\infty(\beta_A),\ e^{X_B/kT} = 16c_\infty(\beta_A)$$
$$\text{and } e^{(X_A+X_B)/kT} = 256\beta_A. \qquad [16]$$

$X_A + X_B$ is the effective single force driving the coupled systems.

I am indebted to Dr. S. R. Caplan for very helpful comments.

1. Hill, T. L. & Chen, Y. (1978) *J. Chem. Phys.* **69**, 1126–1138.
2. Hill, T. L. & Stein, L. (1978) *J. Chem. Phys.* **69**, 1139–1150.
3. Hill, T. L. (1978) *Proc. Natl. Acad. Sci. USA* **75**, 1101–1105.
4. Hill, T. L. (1977) *Proc. Natl. Acad. Sci. USA* **74**, 3632–3636.
5. Hill, T. L. (1977) *Free Energy Transduction in Biology* (Academic, New York).
6. Hill, T. L. & Chance, B. (1978) *J. Theor. Biol.* **72**, 17–56.
7. Hill, T. L. (1977) in *Statistical Mechanics and Statistical Methods in Theory and Application*, ed. Landman, U. (Plenum, New York).
8. Alexandre, A., Reynafarje, B. & Lehninger, A. L. (1978) *Proc. Natl. Acad. Sci. USA* **75**, 5296–5300.
9. Lehninger, A. L. (1975) *Biochemistry* (Worth, New York), 2nd. Ed.
10. Hill, T. L. (1969) *Proc. Natl. Acad. Sci. USA* **64**, 267–274.
11. Hill, T. L. (1970) *Proc. Natl. Acad. Sci. USA* **65**, 409–416.